Chemical Engineering Journal 160 (2010) 615–622

Contents lists available at ScienceDirect

Chemical Engineering Journal

journal homepage: www.elsevier.com/locate/cej

Equilibrium biosorption of lead(II) from aqueous solutions by solid waste from olive-oil production

G. Blázquez*, M. Calero[1], F. Hernáinz[2], G. Tenorio[1], M.A. Martín-Lara[1]

Department of Chemical Engineering University of Granada, 18071 Granada, Spain

ARTICLE INFO

Article history:
Received 13 October 2009
Received in revised form 29 March 2010
Accepted 31 March 2010

Keywords:
Biosorption
Lead
Equilibrium
Wastewater treatment
Solid wastes
Olive-oil production

ABSTRACT

This study examined the lead biosorption capacities of two solid wastes from olive-oil production, two-phase olive mill solid (OMS) and olive stone (OS), using batch experiments at different temperatures. The aim was to determine the isotherms of these wastes and thus their applicability as alternative biosorbents for lead removal. In addition, the solids were characterised by Fourier Transform Infrared (FTIR) spectroscopy.

The OS sorption isotherms were characterised as type I. However, a step characteristic of type IV isotherms was observed in the OMS lead ion sorption isotherms. Well-known non-linear isotherm models, such as Langmuir, Freundlich and Sips, were tested for fit to the OS experimental data, whereas a two-step Langmuir-type model and an adaptation of the Dubinin–Astakov model that can mathematically describe multistep-shaped isotherms were used for the OMS data. The maximum lead uptake was 6.57 mg/g for OS and 23.69 mg/g for OMS at 25 °C. The FTIR spectra before and after lead biosorption, confirmed that carboxyl groups were the main sorption sites for lead removal on the surface of both biosorbents.

1. Introduction

Lead (Pb) is a toxic heavy metal that frequently contaminates aquatic environments. Industrial activities, such as mining and metal processing, can lead to heavy metal contamination in surface water, groundwater, and oceans, causing toxic effects upon entering the food chain [1].

Various techniques have been developed to remove heavy metals from aquatic environments. These include chemical precipitation, ion exchange, activated carbon adsorption, and membrane separation processes. However, these processes may be ineffective or extremely expensive, especially when concentrations of dissolved metal(s) are of the order 1–100 mg/L. Therefore, it is necessary to find new technologies or materials for the removal of heavy metal ions from wastewater.

Biosorption, the ability of certain biomaterials to bind and concentrate heavy metals from even the most dilute aqueous solutions, offers a technically feasible and economically attractive alternative to conventional technologies for the removal of heavy metals from contaminated effluents [2–6].

The metal adsorption capacities of various olive mill solid residues have been investigated in previous studies [7–13]. The disposal of olive mill wastes is a common problem in Mediterranean countries because they pollute soil and water. Olive-oil production is increasing worldwide, with an expected growth rate between 3.5 and 4% per year, according to the International Olive Oil Council.

There are three industrial-scale methods for the extraction of oil from olives, the traditional press-cake system, the three-phase decanter system and the modern two-phase centrifugation system.

This work investigates the Pb(II) removal capacities of two olive-oil production solid wastes, two-phase olive mill solid (OMS) and olive stone (OS). The biosorption process was studied through equilibrium batch experiments. Most sorption isotherms of agricultural wastes are type I. Nevertheless, a step characteristic of type IV isotherms was observed in the OMS lead sorption isotherms. The OS lead biosorption was modelled using one-step models (type I isotherms), which include the Langmuir, Freundlich and Sips isotherms. The OMS equilibrium data were fitted to two-step models (type IV isotherms) using two "new" models proposed in this work, a two-step Langmuir-type model and an adaptation of the Dubinin–Astakov model.

2. Material and methods

2.1. Biosorbent materials

The OS and OMS wastes were provided by the "Cooperativa Nuestra Señora del Castillo" extraction plant located in Vilches,

* Corresponding author. Tel.: +34 958 240770; fax: +34 958 248992.
E-mail addresses: gblazque@ugr.es (G. Blázquez), mcaleroh@ugr.es (M. Calero), hernainz@ugr.es (F. Hernáinz), gtenorio@feugr.ugr.es (G. Tenorio), marianml@ugr.es (M.A. Martín-Lara).
[1] Tel.: +34 958 243311; fax: +34 958 248992.
[2] Tel.: +34 958 243315; fax: +34 958 248992.

1385-8947/$ – see front matter © 2010 Elsevier B.V. All rights reserved.
doi:10.1016/j.cej.2010.03.085

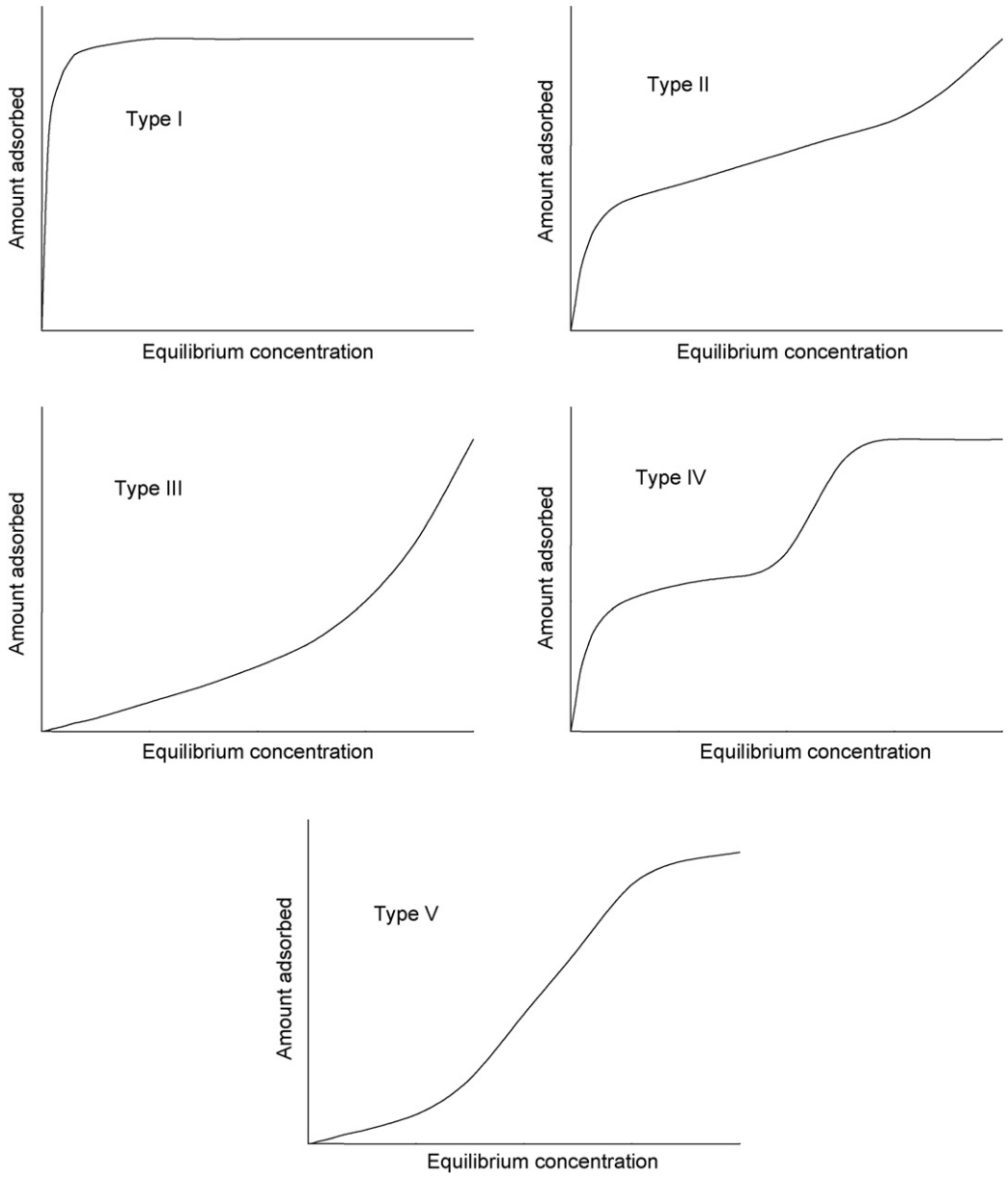

Fig. 1. Illustration of the main characteristic types of sorption isotherms.

in the province of Jaen (Spain). The stones were obtained from olive cake separation with an industrial pitting machine. The OMS waste was collected in sterile plastic containers and refrigerated. This waste is a mixture of pulp and olive stones from the crushing of olives, which yield the oil in a two-phase decanter system. This semi-solid waste contains around 55–60% moisture, has a dark colour, and forms a sludge-like mass. This biosorbent was dried overnight at 60 °C before use in the biosorption experiments. These solids were milled with an analytical mill (IKA MF-10), and the <1.000 mm fraction was chosen for equilibrium batch biosorption tests.

2.2. Equilibrium batch biosorption tests

A 0.5 g sample of biosorbent was added to 50 mL solutions of different Pb^{2+} concentrations (10, 20, 40, 100, 140, 180, 220, 500 and 1000 mg/L) in a 100 mL Erlenmeyer flask. The flasks were shaken at 300 rpm on a shaker at 25, 40 and 60 °C and at pH 5 for 120 min. The solid was then separated by filtration and centrifugation, and the concentration of Pb^{2+} remaining in solution after biosorption was determined using an atomic absorption spectrophotometer (PerkinElmer 3100).

The biosorption capacity at equilibrium time (q_e) was determined according to the following equation:

$$q_e = \frac{(C_i - C_f)V}{m} \quad (1)$$

where C_i and C_f are the initial and final lead concentrations (mg/L) in solution, respectively, V is the solution volume (L) and m is the mass (g) of the biosorbent used.

The stock solutions of Pb(II) were prepared by dissolving appropriate quantities of $Pb(NO_3)_2$ in distilled water and adjusting the solutions to pH 5 with 0.1 M HCl or 0.1 M NaOH. Fresh dilutions were made for each study.

2.3. FTIR spectroscopy

Spectra of native and lead-loaded biosorbents prepared as KBr discs were recorded in an infrared spectrophotometer in the 4000–400 cm^{-1} range. The proportion of biosorbent/KBr was 1/100. The Pb^{2+}-loaded samples were prepared with an initial Pb^{2+} concentration of 10 ppm at pH 5.

2.4. Non-linear regression analysis

All model parameters were evaluated by non-linear regression. In order to evaluate the fit of the equation to the experimental data, the correlation coefficient (R^2) and the squared sum of errors were reported.

3. Results and discussion

3.1. Theoretical aspects of sorption isotherms

When an adsorbate comes into contact with an adsorbent surface, adsorbate molecules adsorb to the surface in quantities that depend on their bulk concentration. A graph of the amount of adsorbate adsorbed over a range of concentrations at a single temperature is known as an adsorption isotherm, or a sorption isotherm. There are many mathematical descriptions of sorption isotherms, some of which are based on a simplified physical picture of sorption and desorption, whereas others are purely empirical and intended to correlate the experimental data in simple equations with two or at most three empirical parameters: the greater the number of empirical parameters, the better the fit to the experimental data [14]. Several different types of isotherms have been presented in the literature; the isotherm shape depends on the type of adsorbent, the type of adsorbate, and intermolecular interactions between the adsorbate and adsorbent. There are five characteristic types of isotherms, as is illustrated in Fig. 1. The sorption isotherms of agricultural wastes generally belong to type I (which has a convex shape). This shape is associated with monomolecular layer adsorption of non-porous or microporous sorbents. Types II and III depict multimolecular adsorption layer formation and strong and weak adsorbate–adsorbent interaction on macroporous adsorbents, respectively. Type IV describes multimolecular layer formation via condensation in mesopores (pore diameter: 2–50 nm), whereas type V describes a similar process, but with both strong and weak adsorbate–adsorbent interactions.

As shown in Fig. 2, the lead ion equilibrium isotherm for OS is a type I isotherm. A step characteristic of type IV isotherms was observed in the biosorption isotherm of lead ions onto OMS.

Several isotherm models are available to describe this equilibrium sorption distribution. In this work, Langmuir, Freundlich and Sips sorption models were used to analyse the lead equilibrium data for OS, and a two-step Langmuir-type model and an adaptation of the Dubinin–Astakov model were used for the OMS data.

3.1.1. Equilibrium models to describe the type I isotherm

3.1.1.1. Langmuir isotherm. The Langmuir isotherm was developed by Irving Langmuir in 1916 to describe the dependence of the surface coverage of an adsorbed gas on the pressure of the gas above the surface at a fixed temperature. The Langmuir isotherm model assumes monolayer adsorption on an energetically homogeneous surface, where the adsorption occurs only at specific localised sites, and saturated coverage corresponds to complete occupancy of these sites. This model can be expressed as follows [15]:

$$q_e = \frac{bq_m C_e}{1 + bC_e} \quad (2)$$

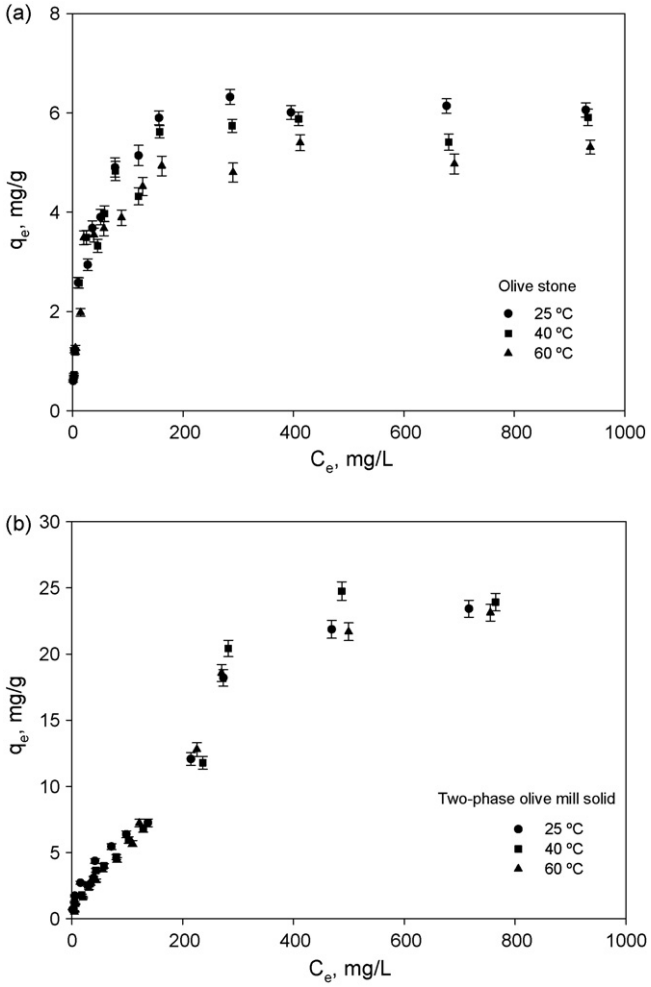

Fig. 2. Lead biosorption isotherms on (a) olive stone and (b) the two-phase olive mill solid at pH 5 and at temperatures of 25, 40 and 60 °C. Error bars indicate standard deviation of duplicate.

where q_e is the amount of metal ion retained per unit of sorbent mass (mg/g), C_e is the equilibrium concentration of metal ion in the liquid phase (mg/L), and q_m and b are the Langmuir constants, related to the maximum sorption capacity for a complete monolayer (mg/g) and to the affinity between the sorbent and sorbate (L/mg), respectively.

As with all chemical reactions, the equilibrium constant b is both temperature-dependent and related to the Gibbs free energy and, hence, to the enthalpy change for the process.

3.1.1.2. Freundlich isotherm. In 1906, Freundlich studied the sorption of a material in coal of animal origin and found a potential relationship between the amount of absorbed solute and the equilibrium concentration, which can be expressed through the following equation [16]:

$$q_e = K_F C_e^{1/n} \quad (3)$$

where q_e and C_e have the same meaning as in the Langmuir isotherm, K_F is the Freundlich sorption constant (mg/g)(L/mg)$^{1/n}$ and n is a constant related to the affinity between the sorbent and the sorbate.

3.1.1.3. Sips isotherm. The Sips model incorporates the features of the Langmuir and Freundlich models into a single equation as fol-

lows [17]:

$$q_e = \frac{q_m b C_e^{1/n}}{1 + b C_e^{1/n}} \quad (4)$$

where q_m, b and n are the Sips constants. The constant n has two limiting behaviours: Langmuir form for $n = 1$ and Freundlich form for very high n values.

3.1.2. Equilibrium models to describe the type IV isotherm

By visual inspection of the lead ion isotherms obtained for OMS, it was concluded that they were characteristic of type IV isotherms. There have been few reports of stepwise shaped isotherms in the field of biosorption [18]. Researchers such as Chubar et al. [19] have found the existence of two capacity zones in the isotherm of copper and zinc on cork biomass. In our work, we presented two mathematical descriptions that described the multistep-shaped isotherms quite well.

3.1.2.1. A two-step Langmuir-type isotherm. In order to explain the type IV isotherm found for lead biosorption by OMS, this work reports the development of a non-linear mathematical model obtained from the sum of two Langmuir-type isotherms, with the assumption that sterically or energetically heterogeneous adsorption sites exist on the biosorbent. Each step on the curve represents different (or identical) types of adsorption sites with different affinities (or availabilities) for lead; the interaction of these sites with lead ions can be described by the Langmuir equation. In this case, the first capacity zone most likely corresponds to the saturation of the sites with a higher affinity for lead (or the saturation of the easily available sites). After this step, increasing the lead concentration in solution initiates the occupation of the sites with less affinity for lead (or the saturation of the less easily available sorption sites). This model contains a critical concentration of the lead ion in solution. Above this concentration, these lower affinity adsorption sites begin to adsorb lead.

$$q_e = \sum_{j=1}^{n} \frac{q_{mi} b_i (C_e - C_i)}{1 + b_i C_e} \quad (5)$$

where C_i is the critical concentration (mg/L), and all other parameters have the same meaning as in the Langmuir isotherm, with the subscript "*i*" used to refer to the stage.

If the isotherm shape results from the fact that the surface of the biosorbent contains the same main sites with different affinities for lead, then a similar constant b must be obtained. In other cases, this shape could result from the existence of different sites that have an active role in the biosorption process.

Finally, to calculate the maximum capacity, it is assumed that the total sorption capacity is the sum of the adsorption capacities of the total effective adsorption sites.

$$q_m = \sum_{i=1}^{n} q_{mi} \quad (6)$$

3.1.2.2. An adaptation of the Dubinin–Astakhov model. This work reports the development of another non-linear mathematical model to elucidate the type IV isotherm found for the lead biosorption by OMS, an adaptation of the Dubinin–Astakov model.

In gas–solid systems, type IV adsorption isotherms are described by two contributions and analysed in terms of the Dubinin–Astakhov equation: the first, at low relative pressures, is type I and the second is type V [20–22].

$$q = q_m \ \exp\left[-\left(\frac{A}{E}\right)^n\right] \quad (7)$$

Table 1
Parameters of the Langmuir, Freundlich and Sips models for Pb(II) biosorption onto OS at 25, 40 and 60 °C.

		Temperature		
		25 °C	40 °C	60 °C
Langmuir: $q_e = \frac{bq_m C_e}{1+bC_e}$	q_m	6.39	5.88	5.25
	b	4.14×10^{-2}	4.73×10^{-2}	5.45×10^{-2}
	R^2	0.999	0.997	0.998
	$\sum(q_e - q_{ecal})^2$	1.49	1.86	1.20
Freundlich: $q_e = K_F C_e^{1/n}$	K_F	1.62	1.56	1.49
	n	4.61	4.73	4.95
	R^2	0.956	0.956	0.968
	$\sum(q_e - q_{ecal})^2$	6.39	6.30	4.88
Sips: $q_e = \frac{q_m b C_e^{1/n}}{1+bC_e^{1/n}}$	q_m	6.57	6.06	5.40
	b	5.73×10^{-2}	6.29×10^{-2}	7.21×10^{-2}
	n	1.13	1.13	1.13
	R^2	0.999	0.998	0.999
	$\sum(q_e - q_{ecal})^2$	1.21	1.68	1.13

where q represents the amount of lead adsorbed at T and P/P_0; q_m is the theoretical maximum capacity; $A = RT\ln(P_0/P)$; and E and n are temperature-invariant parameters of the system.

This paper adapts the Dubinin–Astakov model to the biosorption process (liquid–solid systems) according to the following expression:

$$q_e = q_m \ \exp\left[-\left(\frac{RT\ \ln(1/C)}{E}\right)^n\right] \quad (8)$$

where q_e and q_m are the equilibrium and maximum sorption capacities (mg/g), respectively, R is the gas constant (8.314×10^{-3} kJ/mol K), T is the temperature (K), C is a non-dimensional concentration that represents the ratio between the lead equilibrium concentration in solution, C_e, and the lead saturation concentration, C_s (both in mg/L), n is a non-dimensional parameter and E is the sorption energy (kJ/mol).

The Dubinin–Astakov sorption theory assumes that the sorbent surface has a fixed volume, and sorption potential exists over these sites. The sorption potential is related to an excess of sorption energy over the condensation energy and is independent of temperature. The constant E is related to the mean free energy (kJ/mol) of biosorption per mole of biosorbate when it is transferred to the surface of the solid from solution and provides information about the biosorption mechanism.

3.2. Isotherm modelling of biosorption of lead onto olive stone

The equilibrium modelling related to the biosorption of Pb(II) onto olive stone using the Langmuir, Freundlich and Sips isotherms, their correlation coefficients and residual standard deviations at 25, 40 and 60 °C are reported in Table 1. The graphical correlations between the experimental data and the theoretical models at 25 °C are shown in Fig. 3.

The Langmuir equation provides a reasonable description of the experimental data. This isotherm determines the monolayer capacity of olive stone to be 6.39 mg/g at 25 °C. However, the Sips isotherm exhibits higher R^2 values and lower squared sum of errors values, indicating a considerably better fit compared with the Langmuir isotherm. Although the Sips isotherm best describes the biosorption behaviour of lead ions on olive stone, this isotherm contains three parameters, and the values of n were close to unity, which confirms its tendency towards the Langmuir isotherm. On the other hand, it is obvious that the Freundlich model is less suitable to fit the experimental isotherm curves, as indicated by the low values of the correlation coefficient R^2 and the high values for

Table 2
Parameters of the Langmuir model for Pb(II) biosorption onto OMS at 25, 40 and 60 °C.

		Temperature		
		25 °C	40 °C	60 °C
Step I: $q_e = \frac{q_{m1} b_1 C_e}{1+b_1 C_e}$	q_{m1}	11.0	11.9	12.2
	b_1	1.36×10^{-2}	9.40×10^{-3}	7.60×10^{-3}
	R^2	0.910	0.921	0.884
	$\sum(q_t - q_{tcal})^2$	3.24	0.975	0.401
Step II: $q_e = \frac{q_{m1} b_1 C_e}{1+b_1 C_e} + \frac{q_{m2} b_2 (C_e - C_2)}{1+b_2 C_e}$	q_{m2}	14.3	14.6	12.8
	b_2	2.75×10^{-2}	9.01×10^{-2}	6.60×10^{-2}
	C_2	201	233	217
	R^2	0.999	0.999	0.999
	$\sum(q_t - q_{tcal})^2$	5.64×10^{-2}	1.70	0.140

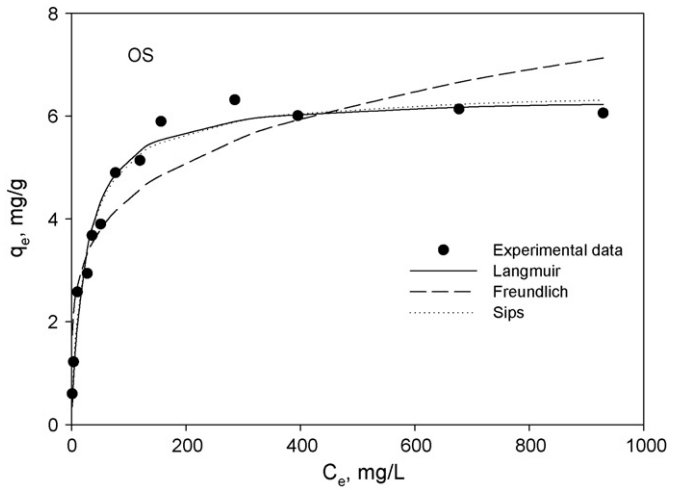

Fig. 3. Experimental biosorption isotherms for lead by OS at pH 5 and 25 °C and their fits to the Langmuir, Freundlich and Sips models.

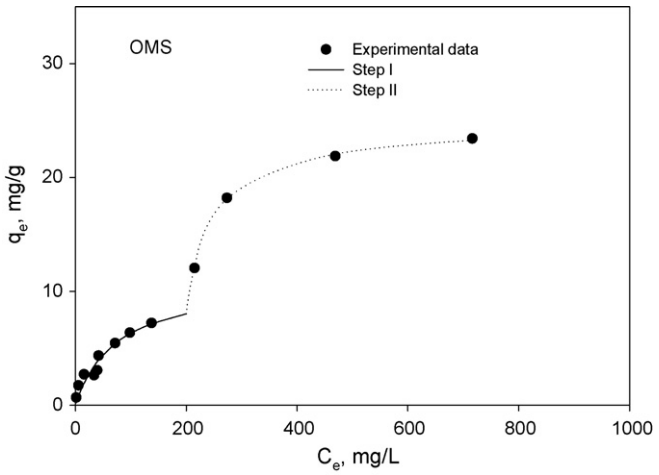

Fig. 4. Experimental biosorption isotherms for lead by OMS at pH 5 and 25 °C and their fits to two consecutive Langmuir isotherms.

the squared sum of errors compared with the Langmuir and Sips models.

With respect to the effect of temperature on lead biosorption equilibrium, these results demonstrate that an increase in temperature results in a lower metal loading per unit weight of the solid. The monolayer capacity q_m for the Langmuir model decreased from 6.39 to 5.25 mg/g for an increase in solution temperature from 25 to 60 °C.

The other monocomponent Langmuir constant b indicates the binding affinity for lead(II) ions. A high b value indicates a high affinity. For olive stone, the affinity for lead increases with temperature.

3.3. Biosorption isotherm modelling of lead onto the two-phase olive mill solid

The OMS equilibrium exhibited characteristics of type IV isotherms (Fig. 2b). The results from the application of the two proposed models are listed in Tables 2 and 3. The graphical correlations between the experimental data and the theoretical models at 25 °C are given in Figs. 4 and 5.

This stepwise behaviour can be explained by the presence of mesopores or by the existence of sites with different affinities for lead that are involved in the OMS lead biosorption process. Horsfall and Spiff [23] found similar results when studying the effects of temperature on the sorption of Pb^{2+} and Cd^{2+} from aqueous solu-

Table 3
Parameters of the Dubinin–Astakov model applied to type I and type V isotherms (step I and step II, respectively) for Pb(II) biosorption onto OMS at 25, 40 and 60 °C.

		Temperature		
		25 °C	40 °C	60 °C
Step I: $q_e = q_{m1} \exp\left[-\left(\frac{RT \ln(1/C)}{E_1}\right)^{n1}\right]$	q_{m1}	10.3	7.45	7.91
	E_1	8.12	9.33	8.76
	n_1	1.71	2.02	1.85
	R^2	0.970	0.980	0.973
	$\sum(q_t - q_{tcal})^2$	2.60	0.426	0.287
Step II: $q_e = q_{m2} \exp\left[-\left(\frac{RT \ln(1/C)}{E_2}\right)^{n2}\right]$	q_{m2}	13.4	17.7	15.2
	E_2	3.71	3.96	4.66
	n_2	3.96	4.30	3.67
	R^2	0.993	0.984	0.990
	$\sum(q_t - q_{tcal})^2$	3.52	11.4	6.05

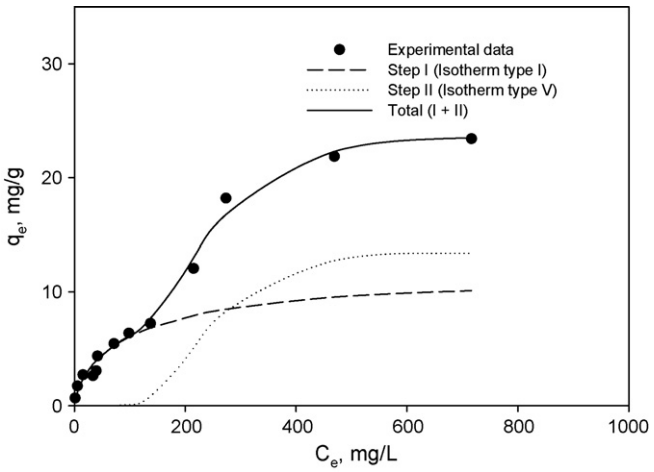

Fig. 5. Experimental biosorption isotherms for lead by OMS at pH 5 and 25 °C and their decomposition into Dubinin–Astakhov isotherms of types I and V.

tion by *Caladium bicolour* (Wild Cocoyam) biomass. This biomass exhibited mixed type I–IV isotherms, and the authors explained this as a characteristic of the biomass substrate, which contains both micropores and mesopores.

For the Dubinin–Astakov model, the type IV lead biosorption isotherms were separated into types I and V contributions, and then each was analysed in terms of the Dubinin–Astakov equation.

Both models provided a good fit to the experimental OMS lead biosorption isotherms. However, the adaptation of the Dubinin–Astakov model seems to provide the best fit to the data. This model provides the highest R^2 values (0.970–0.993) and the lowest values of squared sum of errors for the total curve (first and second steps).

A comparison of the total amount of lead biosorbed by OMS with that biosorbed by OS indicates that the lead biosorption capacity of OMS is about 4 times higher than the reported value for OS at all temperatures (23.7 mg/g versus 6.39 mg/g for OMS and OS at 25 °C, respectively). Additionally, Table 4 presents a comparison between the lead capacities obtained for the sorbents of this work and others found in the literature.

Upon increasing the temperature from 25 to 60 °C, the amount of Pb^{2+} removed from the solution at equilibrium only varies slightly (23.7, 25.1 and 23.1 mg/g at 25, 40 and 60 °C, respectively). Similar results have been reported in the literature; for example, Antunes et al. [34] reported that over a range from 25 to 55 °C, temperature did not significantly affect the biosorption of copper by brown seaweed, *Sargassum* sp. Aderhold et al. [35] reported that temperature fluctuations between 10 and 35 °C did not affect biosorption of copper, cadmium or other heavy metals by the seaweed *E. maxima*. In the two-step Langmuir-type isotherm, the dependence of the critical concentration on the temperature can also be neglected. The first zone ends at a critical lead concentration of approximately 200 mg/L at the three temperatures tested, and increasing the lead concentration in the solution beyond this initiates the second stage. However, in this model, the affinity parameter (parameter *b*) tends to decrease as temperature increases, indicating a decrease in the affinity of OMS for lead at higher temperatures.

Table 4
Comparison between the Pb(II) biosorption capacities of OS, OMS and other biosorbents found in the literature.

Biosorbent	q_m (mg/g)	T (°C)	Reference
Apple residues	17.8	25	[24]
Cocoa shells	6.23	22	[25]
Hazelnut shells	1.78	25	[26]
Coir	18.9	25	[27]
Rice husk	4.00	25	[28]
Oak stem	0.750	25	[29]
Crab shell	19.8	25	[30]
Arca shell	18.3		
Sawdust	21.1	25	[31]
Grape stalks	49.7	25	[32]
Chaff	12.5	25	[33]
Olive stone (OS)	6.39	25	This work
	5.88	40	
	5.25	60	
Two-phase olive mill solid (OMS)	23.7	25	
	25.1	40	
	23.1	60	

However, as indicated before, the value of the constant E (from Dubinin–Astakov) gives some idea of the mean free energy (kJ/mol) of biosorption per mole of biosorbate when it is transferred to the surface of the solid from solution and can give information about the biosorption mechanism. If its value is in the 8–16 kJ/mol range, the biosorption process must follow a chemical ion-exchange mechanism, whereas for values of $E < 8$ kJ/mol, the biosorption process is of a physical nature. The numerical value of the mean free energy of biosorption was 3.71–9.33 kJ/mol, which indicates that the biosorption may occur via a physical process such as electrostatic interaction. For the second part of the lead isotherm, which is type V, a lower E value is obtained than for the initial section (type I). This reflects a less favourable biosorption mechanism [21].

3.4. FTIR analysis

The mechanism of the Pb(II) biosorption by OS and OMS biosorbents was elucidated on the basis of FTIR analysis. To identify the type of Pb(II) binding sites of these solids, the FTIR spectra were recorded before and after lead biosorption and are presented in Fig. 6.

FTIR results revealed very similar spectra for OS and OMS, which confirmed that both have similar functional groups. The spectra have hydroxyl peaks at wave numbers 3411 and 3422 cm^{-1} in OS and OMS, respectively, alkyl peaks at 2927 and 2925 cm^{-1}, peaks at 1740 and 1745 cm^{-1} for the C=O bonds in carboxyl groups and their esters, peaks at 1656 and 1636 cm^{-1} for the asymmetric stretching of the carboxylic C=O double bond, peaks around 1377 and 1380 cm^{-1} attributed to the C–O bond in carboxylic groups, and peaks at 1250 and 1243 cm^{-1} representing the deformation vibration of C=O carboxylic acids. Some peaks in the 1110–1160 and 1040–1060 cm^{-1} range can be attributed to the stretching of the C–O–C and OH of polysaccharides, respectively [32,36–42].

Changes in the FTIR spectra were observed after lead biosorption of the two sorbents. The intensity clearly decreased after Pb^{2+} biosorption, and some peaks shifted to different wave numbers. For example, in the OMS, the absorbance at 1636 cm^{-1} that corresponds to the carboxylic group shifted to 1642 cm^{-1}, indicating the involvement of carboxylic groups in the biosorption process [43,44]. Additionally, the broad stretching absorption bands at 3411 and 3422 cm^{-1} shifted to 3422 and 3415 cm^{-1} for OS and OMS, respectively, although the reason for this shift is unclear. The wave number variation of the 1515 cm^{-1} peak (5 cm^{-1} variation for OMS) has been reported by various authors [38,39,45–49], all of whom attribute it to an amino group. In OMS, the peak at 1243 cm^{-1} shifted to 1260 cm^{-1} (17 cm^{-1} variation), indicating again the involvement of the carboxylic group. For OS, the peak at 1112 cm^{-1} attributed to the stretching of the C–O–C bonds of polysaccharides shifted to 1123 cm^{-1} (11 cm^{-1} variation). Finally, in OMS, the peak at 1075 cm^{-1} disappears. The participation of this peak is referenced in the literature; some authors assign it to alcoholic C–O links [39,46] and others to C–N links [47]. No other significant changes in the absorption lines were observed in the measured range.

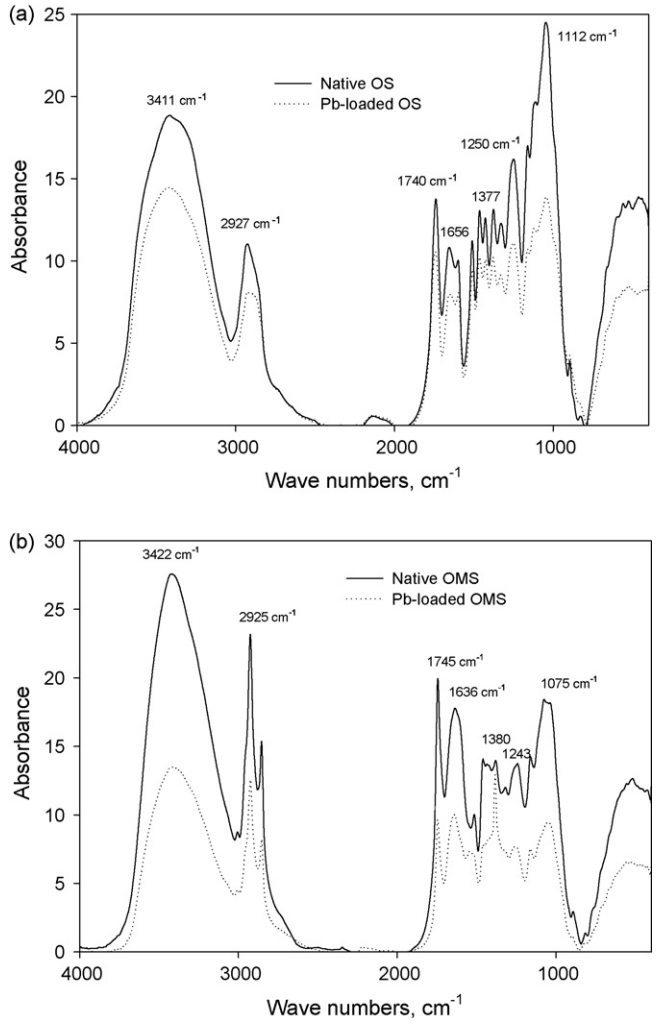

Fig. 6. FTIR spectra of (a) OS and (b) OMS before and after lead biosorption.

It is notable that the intensity variation between FTIR spectra of the samples before and after lead biosorption was lower for OS than for OMS, suggesting a lower retention by OS, which agrees with the lead biosorption capacity values presented above.

4. Conclusions

Due to their low cost, good uptake capacity and short equilibration time, the two solid wastes studied in this work are promising biosorbent materials.

This study indicates two different behaviours for lead biosorption equilibrium related to the nature of the two biosorbents. The Langmuir model is a good isotherm for describing experimental data of OS, and the OMS, which seems to be a mesoporous sorbent, was best described by an adaptation of the Dubinin–Astakov model.

The maximum lead capacities ranged between 6.39–5.25 and 23.7–23.1 mg/g for OS and OMS, respectively, as the temperature increased from 25 to 60 °C.

The FTIR observations indicate that the carboxylic groups present on the sorbents are the binding sites for the lead cations.

Acknowledgement

The authors are grateful to the Ministerio de Educación y Ciencia for the financial support received (Project CTM2005-03957/TECNO) in the realization of this work.

References

[1] S. Schiewer, S.B. Patil, Pectin-rich fruit wastes as biosorbents for heavy metal removal: equilibrium and kinetics, Bioresource Technol. 99 (2008) 1896–1903.
[2] T.A. Davis, B. Volesky, R.H.S.F. Vieira, *Sargassum* seaweed as biosorbent for heavy metals, Water Res. 34 (2000) 4270–4278.
[3] A. Esposito, F. Pagnanelli, A. Lodi, C. Solisio, F. Vegliò, Biosorption of heavy metals by *Sphaerotilus natans*: an equilibrium study at different pH and biomass concentrations, Hydrometallurgy 60 (2001) 129–141.
[4] A. Demir, M. Arisoy, Biological and chemical removal of Cr(VI) from waste water: cost and benefit analysis, J. Hazard. Mater. 147 (2007) 275–280.
[5] B.C. Qi, C. Aldrich, Biosorption of heavy metals from aqueous solutions with tobacco dust, Bioresource Technol. 99 (2008) 5595–5601.
[6] A. Bhatnagar, M. Sillanpää, Utilization of agro-industrial and municipal waste materials as potential adsorbents for water treatment—a review, Chem. Eng. J. 157 (2010) 277–296.
[7] S.H. Gharaibeh, W.Y. Abu-El-Sha'r, M.M. Al-kofahi, Removal of selected heavy metals from aqueous solutions using processed solid residue of olive mill products, Water Res. 32 (1998) 498–502.
[8] F. Pagnanelli, S. Mainelli, F. Vegliò, L. Toro, Heavy metal removal by olive pomace: biosorbent characterisation and equilibrium modelling, Chem. Eng. Sci. 58 (2003) 4709–4717.
[9] F. Pagnanelli, S. Mainelli, S. De Angelis, L. Toro, Biosorption of protons and heavy metals onto olive pomace: modelling of competition effects, Water Res. 39 (2005) 1639–1651.
[10] G. Blázquez, F. Hernáinz, M. Calero, L.F. Ruiz-Núñez, Removal of cadmium ions with olive stones: the effect of some parameters, Process Biochem. 40 (2005) 2649–2654.
[11] M. Calero, F. Hernáinz, G. Blázquez, G. Tenorio, Equilibrium modeling of removal of cadmium ions by olive stone, Environ. Prog. 25 (2006) 261–266.
[12] M.A. Martín-Lara, F. Pagnanelli, S. Mainelli, M. Calero, L. Toro, Chemical treatment of olive pomace: effect on acid-basic properties and metal biosorption capacity, J. Hazard. Mater. 156 (2008) 448–457.
[13] M.A. Martín-Lara, F. Hernáinz, M. Calero, G. Blázquez, G. Tenorio, Surface chemistry evaluation of some solid wastes from olive-oil industry used for lead removal from aqueous solutions, Biochem. Eng. J. 44 (2009) 151–159.
[14] S. Motoyuki, Adsorption Engineering, Elsevier, Tokyo, 1990.
[15] I. Langmuir, The adsorption of gases on plane surfaces of glass, mica and platinum, J. Am. Chem. Soc. 40 (1918) 1361–1403.
[16] H. Freundlich, Colloid and Capillary Chemistry, Methuen, London, UK, 1926.
[17] R. Sips, Structure of a catalyst surface, J. Chem. Phys. 16 (1948) 490–495.
[18] L.N. Konda, I. Czinkota, G. Füleky, G. Morovjan, Modeling of single-step and multistep adsorption isotherms of organic pesticides on soil, J. Agric. Food Chem. 50 (2002) 7326–7331.
[19] N. Chubar, J.R. Carvalho, M.J.N. Correia, Heavy metals biosorption on cork biomass: effect of the pre-treatment, Colloid. Surf. A 238 (2004) 51–58.
[20] M.M. Dubinin, V.A. Astakhov, Description of adsorption equilibria of vapors on zeolites over wide ranges of temperature and pressure, Adv. Chem. 102 (1971) 69–85.
[21] F. Carrasco-Marín, A. Mueden, T.A. Centeno, F. Stoeckli, C. Moreno-Castilla, Water adsorption on activated carbons with different degrees of oxidation, J. Chem. Soc. Faraday Trans. 93 (1997) 2211–2215.
[22] D. Ramirez, S. Qi, M.J. Rood, K.J. Hay, Equilibrium and heat of adsorption for organic vapors and activated carbons, Environ. Sci. Technol. 39 (2005) 5864–5871.
[23] M. Horsfall Jr., A.I. Spiff, Effects of temperature on the sorption of Pb^{2+} and Cd^{2+} from aqueous solution by *Caladium bicolour* (Wild Cocoyam) biomass, Electron. J. Biotechnol. 8 (2005) 43–50.
[24] S.H. Lee, C.H. Jung, H. Chung, M.Y. Lee, J.W. Yang, Removal of heavy metals from aqueous solution by apple residues, Process Biochem. 33 (1998) 205–211.
[25] N. Meunier, J. Laroulandie, J.F. Blais, R.D. Tyagi, Cocoa shells for heavy metal removal from acidic solutions, Bioresource Technol. 90 (2003) 255–263.
[26] G. Cimino, A. Passerini, G. Toscano, Removal of toxic cations and Cr(VI) from aqueous solutions by hazelnut shell, Water Res. 34 (2000) 2955–2962.
[27] K. Conrad, H.C.B. Hansen, Sorption of zinc and lead on coir, Bioresource Technol. 98 (2007) 89–97.
[28] L.B. Khalid, B.S. Girgis, T. Tawfik, Decomposition of H_2O_2 on activated carbon obtained from olive stones, J. Chem. Technol. Biotechnol. 76 (2001) 1132–1140.
[29] M.N.V. Prasad, H. Freitas, Removal of toxic metals from solution by leaf, stem and root phytomass of *Quercus ilex* L. (holly oak), Environ. Pollut. 110 (2000) 277–283.
[30] S. Dahiya, R.M. Tripathi, A.G. Hegde, Biosorption of lead and copper from aqueous solutions by pre-treated crab and arca shell biomass, Bioresource Technol. 99 (2008) 179–187.
[31] Q. Li, J. Zhai, W. Zhang, M. Wang, J. Zhou, Kinetic studies of adsorption of Pb(II), Cr(III) and Cu(II) from aqueous solutions by sawdust and modified peanut husk, J. Hazard. Mater. 141 (2007) 163–167.
[32] M. Martínez, N. Miralles, S. Hidalgo, N. Fiol, I. Villaescusa, J. Poch, Removal of lead (II) and cadmium (II) from aqueous solutions using grape stalk waste, J. Hazard. Mater. 133 (2006) 203–211.
[33] R. Han, J. Zhang, W. Zou, J. Shi, H. Lui, Equilibrium biosorption isotherm for lead ion on chaff, J. Hazard. Mater. 125 (2005) 266–271.
[34] W.A. Antunes, A.S. Luna, C.A. Henriques, A.C. da Costa, An evaluation of copper biosorption by a brown seaweed under optimized conditions, Electron. J. Biotechnol. 6 (2003) 174–184.

[35] D. Aderhold, C.J. Williams, R.G.J. Edyvean, The removal of heavy-metal ions by seaweeds and their derivatives, Bioresource Technol. 58 (1996) 1–6.
[36] S. Deng, Y.P. Ting, Polyethylenimine-modified fungal biomass as a high-capacity biosorbent for Cr (VI) anions: sorption capacity and uptake mechanisms, Environ. Sci. Technol. 39 (2005) 8490–8496.
[37] G. Naja, C. Mustin, B. Volesky, J. Berthelin, A high-resolution titrator: a new approach to studying binding sites of microbial biosorbents, Water Res. 39 (2005) 579–588.
[38] D. Zhou, L. Zhang, S. Guo, Mechanisms of lead biosorption on cellulose/chitin beads, Water Res. 39 (2005) 3755–3762.
[39] S. Sun, L. Wang, A. Wang, Adsorption properties of crosslinked carboxymethyl-chitosan resin with Pb (II) as template ions, J. Hazard. Mater. 136 (2006) 930–937.
[40] K. Bilba, M.A. Arsene, A. Ouensanga, Study of banana and coconut fibers: botanical composition, thermal degradation and textural observations, Bioresource Technol. 98 (2007) 58–68.
[41] A. Çabuk, T. Akar, S. Tunali, S. Gedikli, Biosorption of Pb(II) by industrial strain of *Saccharomyces cerevisiae* immobilized on the biomatrix of cone biomass of *Pinus nigra*: equilibrium and mechanism analysis, Chem. Eng. J. 131 (2007) 293–300.
[42] S. Schiewer, A. Balaria, Biosorption of Pb^{2+} by original and protonated citrus peels: equilibrium, kinetics, and mechanism, Chem. Eng. J. 146 (2009) 211–219.
[43] T. Akar, S. Tunali, I. Kiran, *Botrytis cinerea* as a new fungal biosorbent for removal of Pb(II) from aqueous solutions, Biochem. Eng. J. 25 (2005) 227–235.
[44] P. Lodeiro, J.L. Barriada, R. Herrero, M.E. Sastre de Vicente, The marine macroalga *Cystoseira baccata* as biosorbent for cadmium (II) and lead (II) removal: kinetic and equilibrium studies, Environ. Pollut. 142 (2006) 264–273.
[45] L. Qi, Z. Xu, Lead sorption from aqueous solutions on chitosan nanoparticles, Colloid. Surf. A 251 (2004) 183–190.
[46] P.X. Sheng, Y.-P. Ting, J.P. Chen, L. Hong, Sorption of lead, copper, cadmium, zinc, and nickel by marine algal biomass: characterization of biosorptive capacity and investigation of mechanisms, J. Colloid. Interface. Sci. 275 (2004) 131–141.
[47] S. Deng, Y.-P. Ting, Characterization of PEI-modified biomass and biosorption of Cu (II), Pb (II) and Ni (II), Water Res. 39 (2005) 2167–2177.
[48] S. Tunali, A. Çabuk, T. Akar, Removal of lead and copper ions from aqueous solutions by bacterial strain isolated from soil, Chem. Eng. J. 115 (2006) 203–211.
[49] S. Tunali, T. Akar, S. Özcan, I. Kiran, A. Özcan, Equilibrium and kinetics of biosorption of lead (II) from aqueous solutions by *Cephalosporium aphidicola*, Sep. Purif. Technol. 47 (2006) 105–112.